bank is independent of the filter length. These properties are particularly useful for achieving fast parallel hardware realizations. The parallel module implementation applied to a cosine-modulated filter bank shows that it is decomposed into a parallel set of cosine-modulated module filter banks with fixed small size. The cosine-modulated block filter bank renders a much less restrictive PR condition, and the restriction is so relaxed that most lowpass filters, which have the desired prototype frequency response, satisfy the PR condition. This gives better stopband attenuation for a given design specification and makes the filter design problem much simpler.

REFERENCES

[1] H. Murakami, "Implementation and perfect reconstruction of a maximally decimated FIR filter bank using parallel module decomposition," *IEEE Trans. Signal Processing*, vol. 45, no. 2, pp. 328–332, Feb. 1997.

[2] R. E. Crochiere and L. R. Rabiner, *Multirate Digital Signal Processing*. Englewood Cliffs, NJ: Prentice-Hall, 1983.

[3] H. Murakami, "Block sampling rate conversion systems using real-valued fast cyclic convolution algorithms," *IEEE Trans. Signal Processing*, vol. 45, pp. 1070–1075, Apr. 1997.

[4] P. P. Vaidyanathan, *Multirate Systems and Filter Banks*. Englewood Cliffs, NJ: Prentice-Hall, 1993.

[5] R. D. Koilpillai and P. P. Vaidyanathan, "Cosine-modulated FIR filter banks satisfying perfect reconstruction," *IEEE Trans. Signal Processing*, vol. 40, pp. 770–783, Apr. 1992.

[6] T. Q. Nguyen and R. D. Koilpillai, "The theory and design of arbitrary-length cosine-modulated filter banks and wavelets, satisfying perfect reconstruction," *IEEE Trans. Signal Processing*, vol. 44, pp. 473–483, Mar. 1996.

[7] T. Q. Nguyen, "Near-perfect-reconstruction pseudo-QMF banks," *IEEE Trans. Signal Processing*, vol. 42, pp. 65–76, Jan. 1994.

Performance of Shalvi and Weinstein's Deconvolution Criteria for Channels with/without Zeros on the Unit Circle

Chih-Chun Feng and Chong-Yung Chi

***Abstract*—This correspondence shows that Shalvi and Weinstein's blind deconvolution criteria are applicable for finite SNR regardless of channels having zeros on the unit circle or not. The associated deconvolution filter is stable with a nonlinear relation to the nonblind MMSE equalizer and capable of performing perfect phase equalization for finite SNR.**

***Index Terms*—Blind deconvolution criteria, cumulant, equalization.**

I. INTRODUCTION

Blind deconvolution (equalization) is a signal processing procedure to restore a source signal $u(n)$ from a given set of measurements

$$\begin{aligned} x(n) &= u(n) * h(n) + w(n) \\ &= \sum_{k=-\infty}^{\infty} h(k)u(n-k) + w(n) \end{aligned} \tag{1}$$

Manuscript received May 11, 1998; revised July 21, 1999. This work was supported by the National Science Council under Grant NSC-87-2218-E-007-033. The associate editor coordinating the review of this paper and approving it for publication was Dr. Phillip A. Regalia.

The authors are with the Department of Electrical Engineering, National Tsing Hua University, Hsinchu, Taiwan, R.O.C.

Publisher Item Identifier S 1053-587X(00)00969-7.

where $h(n)$ is an unknown linear time-invariant (LTI) channel, and $w(n)$ is the measurement noise. The blind deconvolution problem occurs in a variety of applications such as communications, seismic exploration, ultrasonic nondestructive evaluation, and speech modeling.

Let $v(n)$ be a deconvolution filter and $e(n)$ be the corresponding deconvolved signal as

$$\begin{aligned} e(n) &= x(n) * v(n) \\ &= u(n) * g(n) + w(n) * v(n) \quad \text{(by (1))} \end{aligned} \tag{2}$$

where

$$g(n) = h(n) * v(n) \tag{3}$$

is the overall system after deconvolution. Shalvi and Weinstein [1] find the optimum $v(n)$ by maximizing the following criteria:

$$J_{p,q}(v(n)) = \frac{|C_{p,q}\{e(n)\}|}{[C_{1,1}\{e(n)\}]^{(p+q)/2}} \tag{4}$$

where both p and q are non-negative integers, $p + q \geq 3$, and $C_{p,q}\{e(n)\}$ denotes the $(p+q)$th-order cumulant of $e(n)$ as

$$C_{p,q}\{e(n)\} = \text{cum}\{\underbrace{e(n), \cdots, e(n)}_{p \text{ terms}}, \underbrace{e^*(n), \cdots, e^*(n)}_{q \text{ terms}}\} \tag{5}$$

in which the superscript "$*$" denotes complex conjugation. The blind deconvolution criteria $J_{p,q}$ include Wiggins' criterion and Donoho's criteria as special cases [1].

It was proved in [1] that maximizing $J_{p,q}$ leads to the overall system $g(n) = \alpha\delta(n-\tau)$, i.e., zero-forcing (ZF) equalization, where α is a scale factor, and τ is a time delay, provided that the signal-to-noise ratio (SNR) equals infinity and the channel $h(n)$ has no zeros on the unit circle, i.e. its inverse system is stable. In practical applications, however, the SNR is always finite, and the behavior of the associated optimum $v(n)$ is accordingly affected by the noise $w(n)$. Moreover, the channel's zeros may be close to or exactly on the unit circle, presenting rather difficult conditions for equalization [2], [3]. In other words, the ZF equalization may no longer be attainable with these practical conditions, and the performance of $J_{p,q}$ thus needs to be further studied. For the case of real signals, Feng and Chi [4] reported a performance analysis of $J_{p,q}$ for finite SNR when $h(n)$ has no zeros on the unit circle. In this correspondence, we extend their analysis to the case of complex signals with $h(n)$ allowed to have zeros on the unit circle. We show that the optimum $v(n)$ associated with $J_{p,q}$ is related to the nonblind minimum mean square error (MMSE) equalizer [5] in a nonlinear manner along with some properties regarding the behavior of $v(n)$. The correspondence is organized as follows. Section II presents some model assumptions, and Section III presents the analytic results about the behavior of $v(n)$ that are then demonstrated through computer simulation in Section IV. Finally, some conclusions are drawn in Section V.

II. MODEL ASSUMPTIONS

For the measurements $x(n)$ given by (1), let us make the following assumptions.

A1) The channel $h(n)$ is stable, i.e., $\sum_n |h(n)| < \infty$, with frequency response $H(\omega) = 0$ for $\omega \in \Omega_Z \subset [-\pi, \pi)$, i.e., $\Omega_Z = \{\omega | H(\omega) = 0, -\pi \leq \omega < \pi\}$.

A2) The source signal $u(n)$ is a zero-mean, independent identically distributed (i.i.d.), non-Gaussian random process with

variance $\sigma_u^2 = C_{1,1}\{u(n)\}$ and $(p+q)$th-order cumulant $\gamma_{p,q} = C_{p,q}\{u(n)\}$ for $p+q \geq 3$.

A3) The noise $w(n)$ is white Gaussian with variance $\sigma_w^2 = C_{1,1}\{w(n)\} > 0$ (i.e. finite SNR) and statistically independent of $u(n)$.

Assumption A1) reveals that when $\Omega_Z \neq \emptyset$ (an empty set), the channel $h(n)$ has zeros on the unit circle and its inverse system is unstable because $1/H(\omega) = \infty$ for $\omega \in \Omega_Z$. This implies that the stable deconvolution filter achieving the ZF equalization does not exist when $\Omega_Z \neq \emptyset$. On the other hand, the (infinite-length) MMSE equalizer given by [6]

$$V_{\mathrm{MSE}}(\omega) = \frac{\sigma_u^2 \cdot H^*(\omega)}{\sigma_u^2 \cdot |H(\omega)|^2 + \sigma_w^2}, \quad \forall \omega \in [-\pi, \pi) \tag{6}$$

is always stable regardless of $\Omega_Z = \emptyset$ or $\Omega_Z \neq \emptyset$ [by (6) and A3)], and meanwhile

$$V_{\mathrm{MSE}}(\omega) = 0, \quad \text{for } \omega \in \Omega_Z \text{ [by (6) and A1)]}. \tag{7}$$

Furthermore, it is a perfect phase equalizer since $\arg[V_{\mathrm{MSE}}(\omega)] = -\arg[H(\omega)]$.

III. Analytic Results

This section analyzes the behavior of the deconvolution filter $v(n)$ associated with $J_{p,q}$ according to A1)–A3). The analytic results for different orders (p and q) of $J_{p,q}$ are quite similar; therefore, only those for $J_{2,2}$ $(p = q = 2)$ are presented for brevity. Note that for the source signal $u(n)$ with symmetric distribution $(p+q)$ must be even; otherwise, $J_{p,q} = 0$ [7].

A. Behavior of the Deconvolution Filter

By (2), A2), and A3), $J_{2,2}$ given by (4) can be expressed as [6], [7]

$$J_{2,2}(v(n)) = \frac{|\gamma_{2,2}| \cdot \sum_n |g(n)|^4}{\left[\sigma_u^2 \sum_n |g(n)|^2 + \sigma_w^2 \sum_n |v(n)|^2\right]^2} \tag{8}$$

which implies the following remark.

R1) $J_{2,2}(v(n)) = J_{2,2}(\alpha v(n-\tau))$ for arbitrary nonzero constant α and arbitrary integer τ.

Then, with regard to the behavior analysis of the deconvolution filter $v(n)$ associated with $J_{2,2}$, let us make the following assumptions for $v(n)$.

B1) The length of $v(n)$ is doubly infinite, implying that finite-length truncation effect of $v(n)$ is not taken into account in the analysis.

B2) $\sum_n |v(n)|^2 < \infty$, implying that $\sum_n |g(n)|^2 < \infty$ [by (3) and A1)]

Assumption B2) also implies the existence of the Fourier transforms $V(\omega)$ and $G(\omega)$, i.e., $|V(\omega)| < \infty$ and $|G(\omega)| < \infty$. Furthermore, it indicates that $C_{1,1}\{e(n)\} = E\{|e(n)|^2\} < \infty$ and the denominator of $J_{2,2}$ given by (8) is accordingly well defined.

On the other hand, it was reported [8] that any nonzero sequence $a(n)$ with finite l_k norm $\{\sum_n |a(n)|^k\}^{1/k}$ satisfies the following inequality:

$$\left\{\sum_n |a(n)|^r\right\}^{1/r} \leq \left\{\sum_n |a(n)|^k\right\}^{1/k} \tag{9}$$

where k and r are positive integers, and $r > k$. Obviously, both $v(n)$ and $g(n)$ have finite l_2 norm by B2). Therefore, by virtue of (9) and B2), we can see that both the numerator and denominator of $J_{2,2}$ given by (8) are finite; therefore, $\sup\{J_{2,2}\} < \infty$ under B2). Next, let us present some properties regarding the behavior of $v(n)$. Taking partial derivative of $J_{2,2}$ given by (8) with respect to $v^*(k)$ and then setting the result to zero, we obtain

$$\beta \cdot \sum_n g^2(n) g^*(n) h^*(n-k) = \sum_n g(n) h^*(n-k) + \frac{\sigma_w^2}{\sigma_u^2} \cdot v(k) \tag{10}$$

where

$$\beta = \frac{\sigma_u^2 \sum_n |g(n)|^2 + \sigma_w^2 \sum_n |v(n)|^2}{\sigma_u^2 \sum_n |g(n)|^4} \tag{11}$$

is a real positive constant. Taking Fourier transform of (10) with respect to the index k yields

$$\beta \cdot D(\omega) H^*(\omega) = G(\omega) H^*(\omega) + \frac{\sigma_w^2}{\sigma_u^2} \cdot V(\omega) = V(\omega) \cdot \left[|H(\omega)|^2 + \frac{\sigma_w^2}{\sigma_u^2}\right] \tag{12}$$

where $D(\omega)$ is the Fourier transform of the sequence

$$d(n) = g^2(n) g^*(n). \tag{13}$$

Then, the following property of $v(n)$ follows directly from (6), (12), and A3).

Property 1: The deconvolution filter associated with $J_{2,2}$ is related to the MMSE equalizer via

$$V(\omega) = \beta \cdot D(\omega) V_{\mathrm{MSE}}(\omega), \quad \forall \omega \in [-\pi, \pi). \tag{14}$$

Property 1 further leads to the following stability property.

Property 2: Under B1) and B2), both the deconvolution filter $v(n)$ and the overall system $g(n)$ associated with $J_{2,2}$ are always stable, regardless of $\Omega_Z = \emptyset$ or $\Omega_Z \neq \emptyset$, and meanwhile

$$V(\omega) = G(\omega) = 0, \quad \text{for } \omega \in \Omega_Z. \tag{15}$$

See Appendix A for the proof. According to (15), a property about the phase response of $V(\omega)$ is as follows.

Property 3: The optimum phase response $\arg[V(\omega)]$ associated with $J_{2,2}$ is given by

$$\arg[V(\omega)] = -\arg[H(\omega)] - \omega\tau + \kappa, \quad \text{for } \omega \in [-\pi, \pi),\ \omega \notin \Omega_Z \tag{16}$$

where τ and κ are constants.

See Appendix B for the proof. This property states that the deconvolution filter $V(\omega)$ completely cancels (or equalizes) the channel-induced phase distortion (up to a time delay τ and a constant phase shift κ) for $\omega \notin \Omega_Z$, and thus, like the MMSE equalizer, it performs as a perfect phase equalizer.

In addition, Property 3 indicates that $G_{\rm ZP}(\omega) = G(\omega)\cdot\exp\{j(\omega\tau-\kappa)\}$ is a zero-phase system and $G_{\rm ZP}(\omega) \geq 0$, thereby leading to the following remark [4], [6].

R2) The impulse response $g_{\rm ZP}(n)$ of $G_{\rm ZP}(\omega)$ is like an autocorrelation function with $g_{\rm ZP}(n) = g^*_{\rm ZP}(-n)$ and $g_{\rm ZP}(0) > |g_{\rm ZP}(n)|$, $\forall n \neq 0$.

This remark reveals that $|g(n)|$ has a unique maximum at the index $n = \tau$ and, meanwhile, is symmetric with respect to $n = \tau$. This result is of particular use to seismic exploration since it accounts for the zero-phase patterns of deconvolved signals in seismic deconvolution [4].

B. Algorithm for Computing the Theoretical Deconvolution Filter

To verify the proposed analytic results, let us present the following FFT-based iterative algorithm for obtaining the theoretical $v(n)$ associated with $J_{2,2}$ from $V_{\rm MSE}(\omega)$ given by (6), according to Property 1.

Algorithm 1:

S1) Set $i = 0$. Choose an initial guess $v^{[0]}(n)$ for $v(n)$.

S2) Set $i = i + 1$. Compute the L-point DFT $V^{[i-1]}(\omega_k = 2\pi k/L)$, of $v^{[i-1]}(n)$. Compute $G^{[i-1]}(\omega_k) = H(\omega_k)\cdot V^{[i-1]}(\omega_k)$, and then, compute its L-point inverse DFT $g^{[i-1]}(n)$.

S3) Compute $d(n)$ using (13) with $g(n) = g^{[i-1]}(n)$, and then, compute its L-point DFT $D(\omega_k)$.

S4) Compute $\widetilde{V}(\omega_k) = D(\omega_k)\cdot V_{\rm MSE}(\omega_k)$ [see (14)], and then, compute its L-point inverse DFT $\tilde{v}(n)$. Compute $v^{[i]}(n) = \tilde{v}(n)/\sqrt{\sum_n |\tilde{v}(n)|^2}$ [due to R1)].

S5) If $\sum_n |v^{[i]}(n) - v^{[i-1]}(n)|^2 > \epsilon$ (a preassigned tolerance for convergence), then go to S2); otherwise, the theoretical $v(n) = v^{[i]}(n)$ is obtained.

Note that Algorithm 1 is not an algorithm to design the deconvolution filter $v(n)$ from the data $x(n)$. It requires exact knowledge about the channel response $H(\omega)$ and the ratio σ_u^2/σ_w^2 [see S2), S4) and (6)] but is never limited by the length of $v(n)$ as long as the DFT length L is chosen sufficiently large so that aliasing effects on the resultant $v(n)$ are negligible. Next, let us show some simulation results to verify the preceding analytic results.

IV. Computer Simulation

In the simulation, the source signal $u(n)$ was assumed to be a four-QAM signal, and the channel $h(n)$, which was plotted in Fig. 1, was taken from [2] as $H(z) = H_1(z)\cdot H_2(z)$, where $H_1(z)$ and $H_2(z)$ were causal FIR filters with coefficients $\{1, 0, -1\}$ and $\{0.04, -0.05, 0.07, -0.21, -0.5, 0.72, 0.36, 0, 0.21, 0.03, 0.07\}$, respectively. Fig. 1(a) and (b) exhibit that $|H(\omega = 0)| = |H(\omega = \pm\pi)| = 0$, and ARG$[H(\omega)]$ has a discontinuity of π at $\omega = 0$ and a discontinuity of $-\pi$ at $\omega = \pm\pi$ due to the two zeros of $H_1(z)$ on the unit circle ($z = \pm 1$). The deconvolution filter $v(n)$ was approximated by a 30th-order causal FIR filter $\widehat{v}(n)$, and an iterative gradient-type optimization algorithm with initial condition $\hat{v}(n) = \delta(n - 15)$ was used to find the maximum of $J_{2,2}$ as well as the relevant estimate $\hat{v}(n)$. Then, the average $\hat{v}_{\rm ave}(n)$ of 30 $\hat{v}(n)$'s from 30 independent runs was obtained with data length equal to 8000 and the SNR equal to 20 dB (complex white Gaussian noise). On the other hand, the theoretical $v(n)$ was obtained using Algorithm 1 with the initial guess $v^{[0]}(n) = \delta(n)$, DFT length $L = 1024$, and convergence tolerance $\epsilon = 10^{-5}$. The simulation results are displayed in Fig. 2, where scale factors and time delays were artificially removed. Fig. 2(a) exhibits that $v(n)$ may be approximated well by a long-length FIR filter $\hat{v}(n)$ of order equal to about 80 and that the theoretical $v(n)$ obtained by Algorithm 1 can serve as a prediction for $\hat{v}(n)$. Additionally, we can see from Fig. 2(b), Fig. 2(c), and Fig. 1(b) that $|V(\omega = 0)| = |V(\omega = \pm\pi)| = 0$ and ARG$[V(\omega)] = -$ARG$[H(\omega)]$ and that both $|\hat{V}_{\rm ave}(\omega)|$ and ARG$[\hat{V}_{\rm ave}(\omega)]$ are close to $|V(\omega)|$ and ARG$[V(\omega)]$, respectively, except for those around $\omega = 0$ and $\pm\pi$. The large magnitude and phase errors around $\omega = 0$ and $\pm\pi$ in Fig. 2(b) and (c) result from the low magnitude of $H(\omega)$ around these frequencies [see Fig. 1(a)] or, equivalently, the low signal power of these frequency components in the data $x(n)$. As a consequence, the results in Fig. 2(a)–(c) confirm Properties 1 through 3.

Fig. 2(d) exhibits that $|\hat{g}_{\rm ZP}(n)|$ is quite close to $|g_{\rm ZP}(n)|$ and approaches $\delta(n)$ implying that $\hat{v}(n)$ performs intersymbol interference

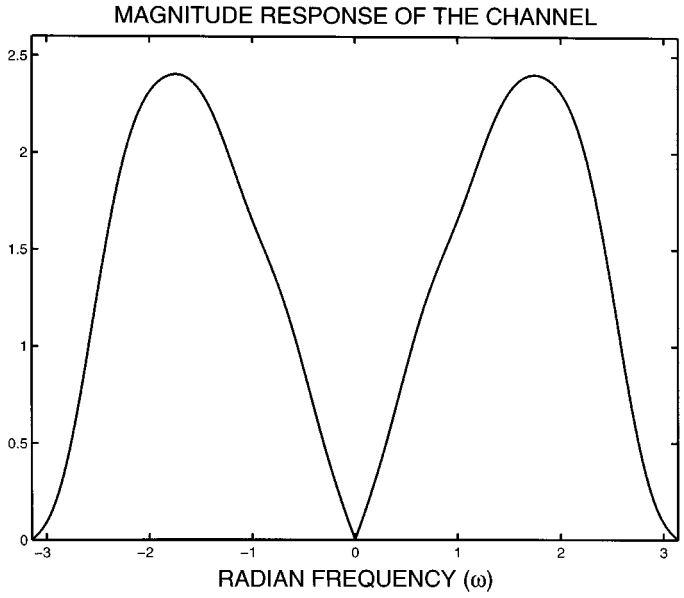

(a)

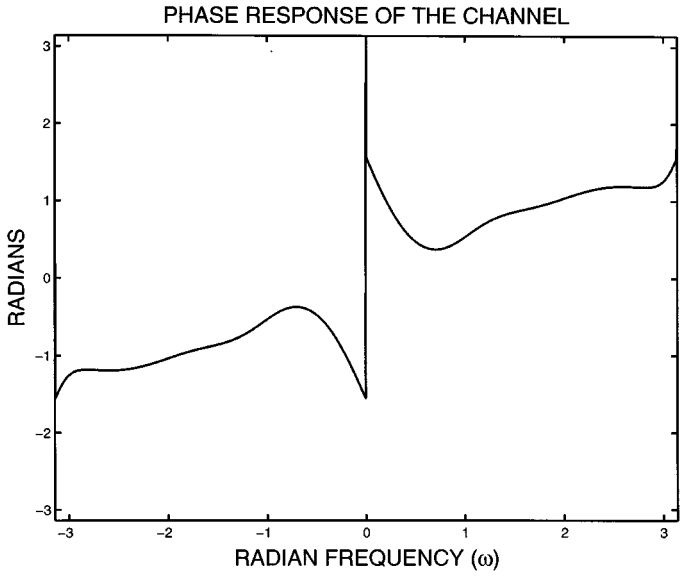

(b)

Fig. 1. (a) Magnitude response $|\boldsymbol{H(\omega)}|$ and (b) principal value ARG$[\boldsymbol{H(\omega)}]$ of the phase response $\arg[\boldsymbol{H(\omega)}]$ of the channel $\boldsymbol{h(n)}$ for $\boldsymbol{\omega \in [-\pi, \pi]}$, where a linear phase term in (b) was removed for clarity.

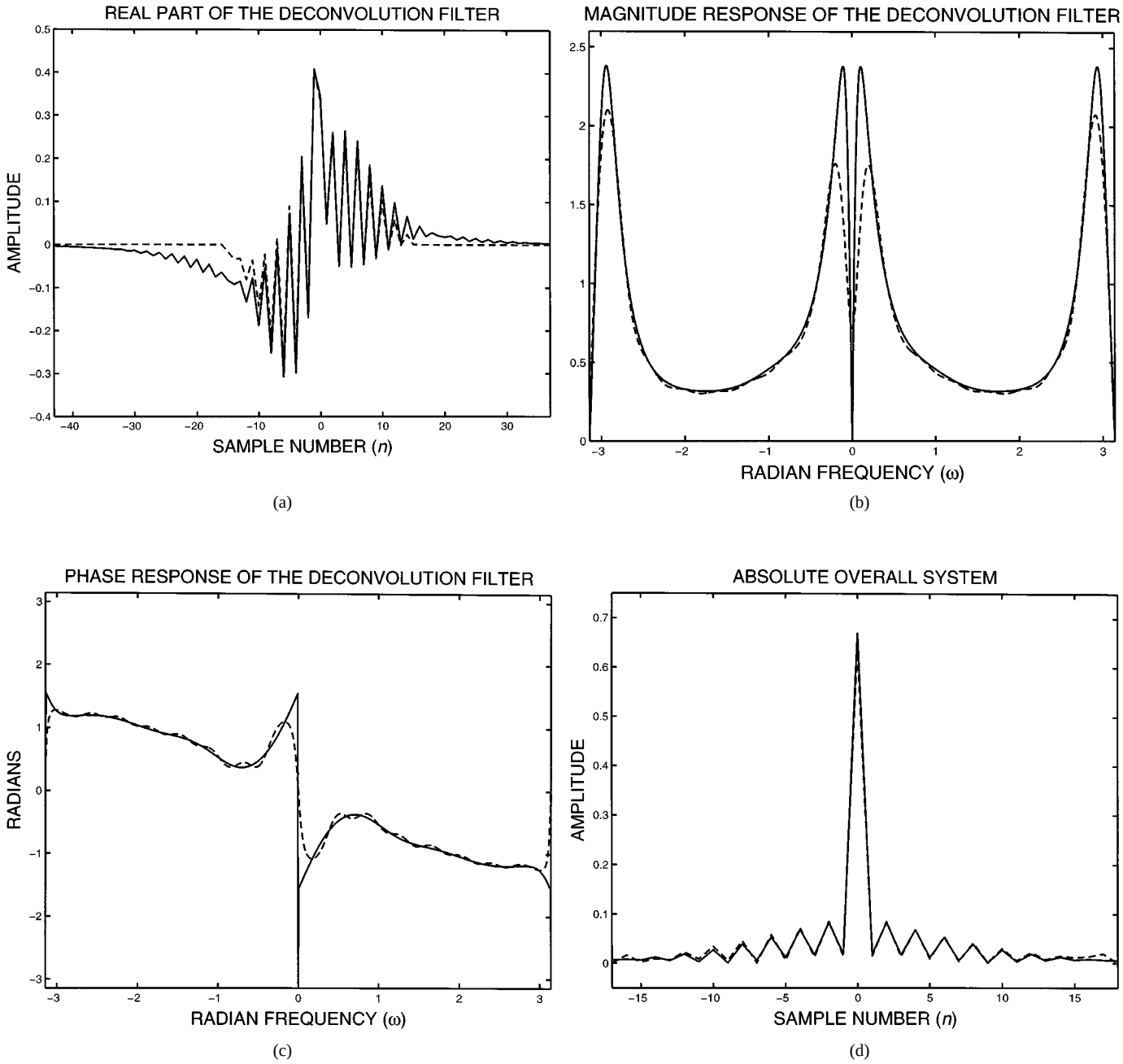

Fig. 2. (a) Real parts, (b) magnitude responses, and (c) phase responses (principal values) of the obtained estimate $\hat{\boldsymbol{v}}_{\rm avc}(\boldsymbol{n})$ (dashed lines) and the theoretical $\boldsymbol{v}(\boldsymbol{n})$ (solid lines), while their imaginary parts are not displayed since they are almost zero. (d) Corresponding absolute zero-phase overall system estimate $|\hat{\boldsymbol{g}}_{\rm ZP}(\boldsymbol{n})|$ (dashed line) and theoretical zero-phase overall system $|\boldsymbol{g}_{\rm ZP}(\boldsymbol{n})|$ (solid line).

(ISI) reduction well for this case. Moreover, $|\hat{g}_{\rm ZP}(n)|$ is approximately symmetric with $|\hat{g}_{\rm ZP}(0)| > |\hat{g}_{\rm ZP}(n)|$, $n \neq 0.$, which is consistent with R2).

V. Conclusions

The proposed analytic results about the performance of the blind deconvolution criteria $J_{p,q}$ given by (4) include the connection of the associated deconvolution filter $v(n)$ with the nonblind MMSE equalizer, guaranteed stability of $v(n)$ regardless of the locations of the channel's zeros and capability of perfect phase equalization for finite SNR, as summarized in Properties 1 through 3. These analytic results are helpful to realizing the behavior of $v(n)$ associated with $J_{p,q}$.

Appendix A
Proof of Property 2

From (9), (11) and B2), we can easily show that $\beta < \infty$. By (14) and $\beta < \infty$, we can infer that if $d(n)$ is stable, then $v(n)$ is stable since $v_{\rm MSE}(n)$ is stable. Invoking (9), (13), and B2), we obtain $\sum_n |d(n)| \leq \left\{\sum_n |g(n)|^2\right\}^{3/2} < \infty$. This, therefore, completes the proof that $v(n)$ is stable, and so is $g(n)$ by A1). Then, (15) follows directly from (3), (7), and (14).

APPENDIX B
PROOF OF PROPERTY 3

Let $\Phi(\omega) \triangleq \arg[G(\omega)] = \arg[H(\omega)] + \arg[V(\omega)]$. The denominator of $J_{2,2}$ given by (8) can be easily shown to be independent of $\arg[V(\omega)]$, whereas the numerator of $J_{2,2}$ can be shown to be [7]

$$\begin{aligned}
&|C_{2,2}\{e(n)\}| \\
&\quad = \left| \frac{1}{(2\pi)^3} \int_{-\pi}^{\pi}\int_{-\pi}^{\pi}\int_{-\pi}^{\pi} \gamma_{2,2} \right. \\
&\qquad \cdot |G(-\omega_1+\omega_2+\omega_3)| \cdot \prod_{i=1}^{3} |G(\omega_i)| \\
&\qquad \cdot \exp\left\{ j\left[\Phi(-\omega_1+\omega_2+\omega_3)\right.\right. \\
&\qquad \left.\left. + \Phi(\omega_1) - \Phi(\omega_2) - \Phi(\omega_3)\right]\right\} d\omega_1\, d\omega_2\, d\omega_3 \Bigg| \\
&\quad \le \frac{|\gamma_{2,2}|}{(2\pi)^3} \int_{-\pi}^{\pi}\int_{-\pi}^{\pi}\int_{-\pi}^{\pi} |G(-\omega_1+\omega_2+\omega_3)| \\
&\qquad \cdot \prod_{i=1}^{3} |G(\omega_i)| d\omega_1\, d\omega_2\, d\omega_3. \qquad \text{(B.1)}
\end{aligned}$$

Due to (15), the equality of (B.1) requires that $[\Phi(-\omega_1+\omega_2+\omega_3) + \Phi(\omega_1) - \Phi(\omega_2) - \Phi(\omega_3)]$ be equal to a constant for $-\omega_1+\omega_2+\omega_3 \notin \Omega_Z$ and $\omega_i \notin \Omega_Z$, $i = 1, 2, 3$. This implies that the optimum $\Phi(\omega)$ associated with the maximum of $J_{2,2}$ is linear for $\omega \in [-\pi, \pi)$ and $\omega \notin \Omega_Z$., and thus, the optimum $\arg[V(\omega)]$ is as given by (16), regardless of what $|V(\omega)|$ for $\omega \in [-\pi, \pi)$ and $\omega \notin \Omega_Z$ is.

ACKNOWLEDGMENT

The authors would like to thank the anonymous reviewers and the associate editor for their valuable comments and suggestions on the improvement of this correspondence. They also thank C.-H. Hsi for his assistance in deriving an earlier version of Property 1.

REFERENCES

[1] O. Shalvi and E. Weinstein, *Universal Methods for Blind Deconvolution, A chapter in Blind Deconvolution*, S. Haykin, Ed. Englewood Cliffs, NJ: Prentice-Hall, 1994.
[2] J. K. Tugnait and U. Gummadavelli, "Blind equalization and channel estimation with partial response input signals," *IEEE Trans. Commun.*, vol. 45, pp. 1025–1031, Sept. 1997.
[3] I. Fijalkow, "Multichannel equalization lower bound: A function of channel noise and disparity," in *Proc. IEEE SP Workshop SSAP*, Corfu, Greece, June 26, 1996, pp. 344–347.
[4] C.-C. Feng and C.-Y. Chi, "Performance of cumulant based inverse filters for blind deconvolution," *IEEE Trans. Signal Processing*, vol. 47, July 1999.
[5] J. G. Proakis, *Digital Communications*. New York: McGraw-Hill, 1995.
[6] M. H. Hayes, *Statistical Digital Signal Processing and Modeling*. New York, NY: Wiley, 1996.
[7] C. L. Nikias and A. P. Petropulu, *Higher-Order Spectra Analysis: A Nonlinear Signal Processing Framework*. Englewood Cliffs, NJ: Prentice-Hall, 1993.
[8] G. H. Hardy, J. E. Littlewood, and G. Polya, *Inequalities*. London, U.K.: Cambridge Univ.Press, 1934.

Blind Source Separation Using Clustering-Based Multivariate Density Estimation Algorithm

Zhenya He, Luxi Yang, Ju Liu, Ziyi Lu, Chen He, and Yuhui Shi

***Abstract*—A learning algorithm is developed for blind separation of the independent source signals from their linear mixtures. The algorithm is based on minimizing a contrast function defined in terms of the Kullback–Leibler distance. We use a clustering-based multivariate density estimation approach to reduce the number of the parameters to be updated. Simulations illustrate the validity of the algorithm.**

I. INTRODUCTION

Blind source separation (BSS), which is also known as the independent component analysis (ICA), has received much attention recently in the signal processing field [1]–[5], [9]–[16] and has found many important applications. Generally speaking, the problem of BSS can be formulated as the problem of separating or estimating waveforms of primary sources from their linear mixtures, without knowing the characteristics of the transmission channels. In the simplest case, we see N sequences $X_1(t), X_2(t), \cdots, X_N(t)$ recorded from N different sensors, each observation $X_i(t)$ being a linear combination of M independent sources $S_1(t), S_2(t), \cdots, S_M(t)$. Thus, $X(t) = AS(t)$, where $X(t)$ and $S(t)$ denote the vectors $X_1(t), X_2(t), \cdots, X_N(t)$ and $S_1(t), S_2(t), \cdots, S_M(t)$, respectively. A is a $N \times M$ matrix. The BSS problem is to find an $M \times N$ matrix W only from the observations $X(t)$ such that the output $Y(t) = WX(t)$ is as close as possible to the source signals $S(t)$.

Currently, there exist several types of approaches to solve such a problem. The seminal work is by Jutten and Herault [1]. Their heuristic algorithm, which is inspired by a neuromimetic approach, is attractive because it is simple and can be realized locally, but it fails in separating more than two independent sources. Karhunen [4], [9] found that nonlinear Hebbian learning in a self-organizing neural network can perform independent component analysis and can thus solve the source separation problem. The most critical factor of this approach is how to select a proper contrast function [2], [3], [12]. A few new neural separating algorithms have been derived from several contrast functions based on information theoretic concepts. Pham [11] and Amari [3] proposed separating algorithms based on the Kullback–Leibler distance. Pham [11] gave the choice of a marginal density function, which is important for the separating algorithms to perform well. He estimated the density through a kernel method with implicit data prewhitening. He also computed the Hessian and implemented a Gauss–Newton type algorithm that has faster convergence. Bell and Sejnowski [5] derived a separating algorithm that maximizes the information transferred in a network of nonlinear units. Bell's algorithm actually is also based on Kullback–Leibler distance. Obradovic and Deco[19] pointed out that the separating algorithms based on Kullback–Leibler distance and Bell's Infomax algorithm lead to the same solution if the parameterization of the output nonlinear functions in the latter method is sufficiently rich. Comon [2] proposed a cumulant-based approach. Deco and Obradovic [18] extended the approach by defining a parameterization by rotation matrices.

Manuscript received September 25, 1998; revised July 12, 1999. This work was supported by "Climbing Program—National Key Project for Fundamental Research in China." The associate editor coordinating the review of this paper and approving it for publication was Dr. Alle-Jan van der Veen.

The authors are with the Radio Engineering Department, Southeast University, Nanjing, China.

Publisher Item Identifier S 1053-587X(00)00986-7.